Supplementary materials

Croconic Acid Doped Glycine Single Crystals: Growth, Crystal Structure, UV-Vis, FTIR, Raman and Photoluminescence Spectroscopy

Elena Balashova[1*], Aleksandr A. Levin[1], Valery Davydov[1], Alexander Smirnov[1], Anatoly Starukhin[1], Sergei Pavlov[1], Boris Krichevtsov[1], Andrey Zolotarev[2], Hongjun Zhang[3], Fangzhe Li[3], Hua Ke[3]

1 Ioffe Institute, Politechnicheskaya 26, 194021 Saint Petersburg, Russia; aleksandr.a.levin@mail.ioffe.ru (A.A.L.); Valery.Davydov@mail.ioffe.ru (V.Y.D.); Alex.Smirnov@mail.ioffe.ru (A.N.S.); boris@mail.ioffe.ru (B.B.K.); A.Starukhin@mail.ioffe.ru (A.N.S.); Pavlov_sergey@mail.ioffe.ru (S.I.P.)
2 Saint-Petersburg State University, Saint-Petersburg 199034, Russia, a.zolotarev@spbu.ru (A.A.Z.)
3 Harbin Institute of Technology, Harbin 150080, China; zhanghj@hit.edu.cn (H.Zh.); lifangzhe@hit.edu.cn (F.L.); hua_ke@hit.edu.cn (H.K.)
* Correspondence: balashova@mail.ioffe.ru

S1. Single crystal XRD

Table S1. Results of refinement of the α-Gly:CA(90:10) structure (space group $P2_1/n$ (14)) using single crystal XRD data. Wyckoff positions, atomic numbers Z, relative coordinates of atoms (*x*/*a*, *y*/*b*, *z*/*c*), and their equivalent/isotropic temperature factors $U_{eq/iso}$ are shown. Numbering of atoms in first column (Atom) corresponds to CIF file and in second colomn (Atom [1]) to Ref. [1].

Atom	Atom [1]	Wyckoff position	*Z*	*x*/*a*	*y*/*b*	*z*/c	$U_{eq/iso}$, Å^2 [a]
O2	O2	4*e*	8	0.8055(2)	0.59427(10)	0.7354(2)	0.0414(4)
O1	O1	4*e*	8	0.3527(3)	0.64165(11)	0.6069(2)	0.0451(4)
N1	N1	4*e*	7	0.8011(3)	0.59006(12)	0.2408(3)	0.0378(4)
H1A	H3	4*e*	1	0.784721	0.601259	0.074576	0.045
H1B	H4	4*e*	1	0.797635	0.517054	0.270641	0.045
H1C	H5	4*e*	1	0.963541	0.618741	0.349371	0.045
C1	C1	4*e*	6	0.5758(3)	0.62490(13)	0.5670(3)	0.0333(4)
C2	C2	4*e*	6	0.5646(4)	0.64497(14)	0.2871(3)	0.0356(4)
H2A	H1	4*e*	1	0.387612	0.616507	0.161971	0.043
H2B	H2	4*e*	1	0.570929	0.724688	0.257577	0.043

[a] Equivalent isotropic temperature factors U_{eq} are shown for non-hydrogen atoms refined in an approximation of anisotropic temperature factor. For atoms of H, the isotropic temperature factors U_{iso} are shown.

Symmetry codes:

x, *y*, *z*

-*x*+1/2, *y*+1/2, -*z*+1/2

-*x*, -*y*, -*z*

x-1/2, -*y*-1/2, *z*-1/2

Table S2. Atomic displacement parameters (U^{ij}, Å) for the α-Gly:CA(90:10) (Å²).

Atom	U^{11}	U^{22}	U^{33}	U^{23}	U^{13}	U^{12}
O2	0.0416(8)	0.0528(8)	0.0314(7)	0.0036(5)	0.0152(6)	0.0060(5)
O1	0.0382(7)	0.0617(9)	0.0409(7)	-0.0038(6)	0.0210(6)	0.0007(6)
N1	0.0386(8)	0.0472(8)	0.0293(7)	0.0018(6)	0.0146(6)	0.0041(6)
C1	0.0376(9)	0.0312(8)	0.0334(9)	-0.0023(6)	0.0157(7)	-0.0033(6)
C2	0.0347(8)	0.0406(8)	0.0331(9)	0.0032(7)	0.0145(7)	0.0034(6)

Table S3. Results of refinement of the γ-Gly:CA(80:20) structure (space group $P3_1$ (N 144)) using single crystal XRD data. Atomic numbers Z, relative coordinates of atoms (x/a, y/b, z/c) and their equivalent/isotropic temperature factors $U_{eq/iso}$ are shown. Numbering of atoms in first column (Atom) corresponds to CIF file and in second colomn (Atom [1]) to Ref. [1].

Atom	Atom [1]	Wyckoff position	*Z*	*x/a*	*y/b*	*z/c*	$U_{eq/iso}$(Å²) [a]
O001	O2	3*a*	8	0.5538(4)	0.6543(4)	0.2728(4)	0.0142(4)
O002	O1	3*a*	8	0.8805(4)	0.6702(4)	0.2414(4)	0.0182(5)
C003	C1	3*a*	6	0.7276(5)	0.6691(5)	0.3604(5)	0.0129(5)
N004	N1	3*a*	7	0.5502(4)	0.6394(4)	0.7627(5)	0.0133(5)
H00A	H3	3*a*	1	0.503610	0.733629	0.713027	0.016
H00B	H4	3*a*	1	0.573370	0.652301	0.926942	0.016
H00C	H5	3*a*	1	0.445380	0.498071	0.725872	0.016
C005	C2	3*a*	6	0.7588(5)	0.6947(6)	0.6364(5)	0.0154(6)
H00D	H1	3*a*	1	0.812898	0.596533	0.696507	0.018
H00E	H2	3*a*	1	0.872097	0.848977	0.675272	0.018

[a] Equivalent isotropic temperature factors U_{eq} are shown for non-hydrogen atoms refined in an approximation of anisotropic temperature factor. For atoms of H, the isotropic temperature factors U_{iso} are shown.

Symmetry codes xyz:

'x, y, z'

'-y, x-y, z+1/3'

'-x+y, -x, z+2/3'

Table S4. Atomic displacement parameters (U^{ij}, Å) for the γ-Gly:CA(80:20) (Å²).

Atom	U^{11}	U^{22}	U^{33}	U^{23}	U^{13}	U^{12}
O2	0.0142(11)	00.0190(10)	0.0104(8)	-0.0005(11)	-0.0017(10)	0.0091(9)
O1	0.0186(12)	0.0261(12)	0.0154(10)	0.0026(10)	0.0028(10)	0.0153(11)
N1	0.0147(13)	0.0156(13)	0.0103(9)	-0.0027(11)	-0.0023(11)	0.0081(10)
C1	0.0155(14)	0.0121(14)	0.0113(11)	0.0001(12)	-0.0005(12)	0.0071(13)
C2	0.0128(14)	0.0194(16)	0.0131(14)	-0.0001(12)	-0.0003(10)	0.0075(15)

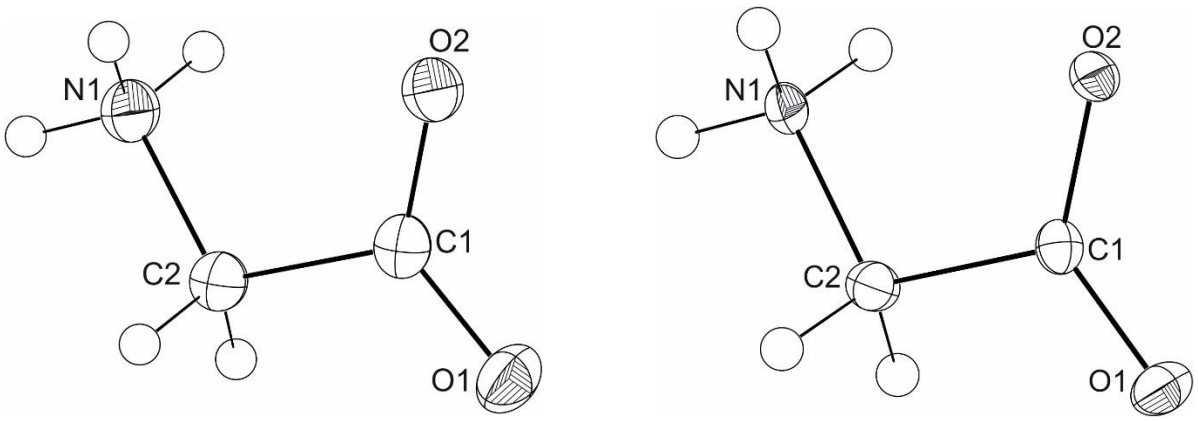

(a) **(b)**

Figure S1. Glycine molecule in (a) α-Gly:CA(90:10) and (b) γ-Gly:CA(80:20) with atoms represented by thermal ellipsoids by means of program ORTEP [2] using the data presented in Tables S1−S2 and S3−S4, correspondingly. Numbering of atoms corresponds to Ref. [1].

S2. Powder XRD

Williamson-Hall plot (WHP) and size-strain plot (SSP), Le Bail (LB) and Rietveld analysis of the samples was carried out (Figures S2 and S3).

In WHP, SSP, LB and Rietveld techniques, the same coefficients of Scherrer ($K_{Scherrer}$ = 0.94) and Wilson-Stokes (K_{strain} = 4) equations, connecting the XRD reflection broadening with crystallite size and microstrain, correspondingly. In the Figures S2 and S3, the mean values of the criterion $FWHM/B_{int}$ averaged over all observed reflections taken into account in the WHP/SSP calculations are shown, evidencing the pseudo-Voigt (pV) type of XRD reflection profiles (there, $FWHM = FWHM_{obs}$ is observed full width at half maximum of the XRD reflections, $B_{int} = I_{int}/I_{max}$ is the observed integral width of the XRD reflections, I_{max} and I_{int} are maximum and integral reflection intensities, respectively). As well as the coefficient of determination of R_{cod} (see References. [3, 4] for definition) is presented in Figures S2 and S3. This coefficient is a measure of how well the experimental points fit on a straight line (R_{cod} = 0% means very bad, and R_{cod} = 100% means perfect).

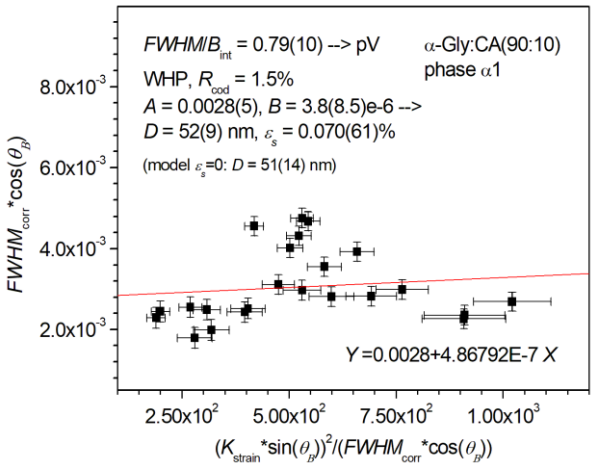

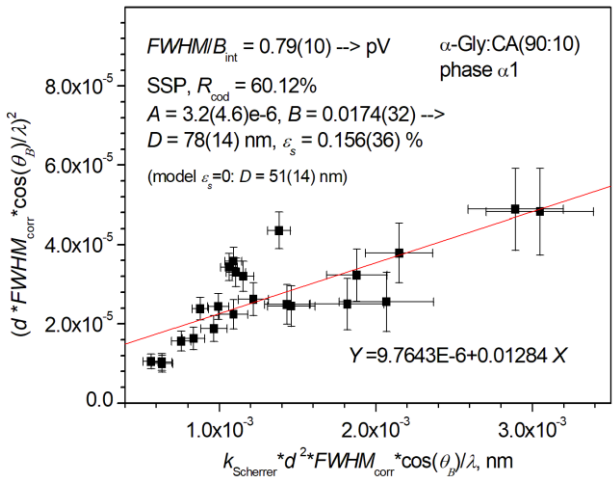

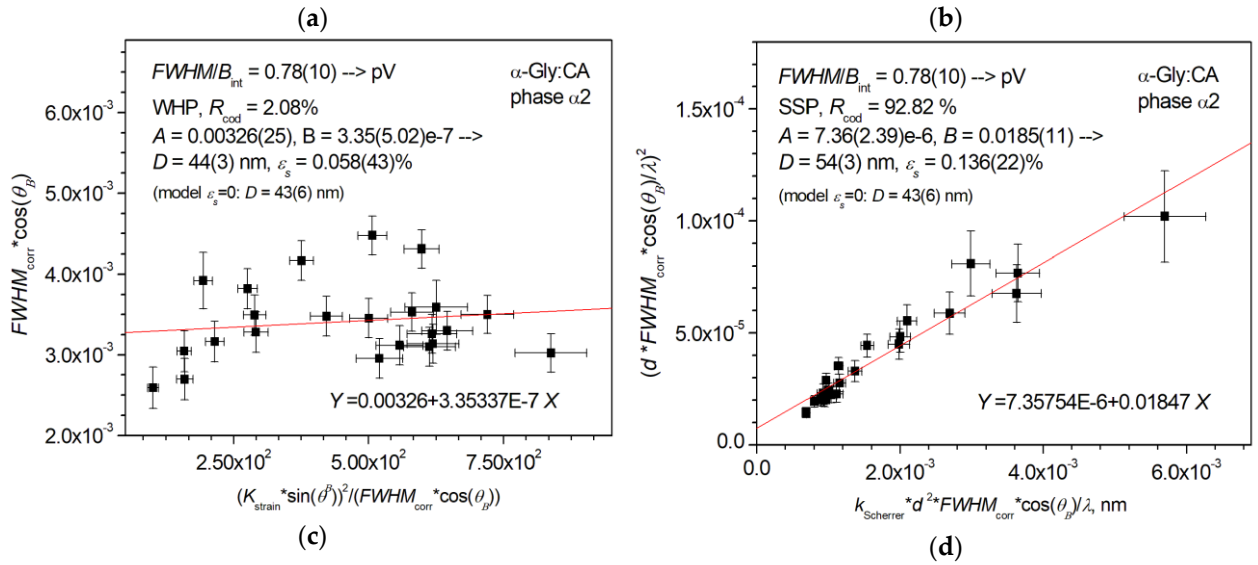

Figure S2. (**a**), (**c**) WHP and (**b**), (**d**), (**f**) SSP of α1 and α2 modifications of α-Gly. $FWHM_{corr}$ is full width at half maximum of the XRD reflection corrected to instrumental broadening, θ_B is half of Bragg angle $2\theta_B$ of the reflection after angular corrections applied, d is interplane distance corresponding to Bragg angle $2\theta_B$ of the reflection, λ is the wave length of Cu-$K_{\alpha 1}$ radiation (1.540598 Å, after correction of Cu-$K_{\alpha 2}$ contribution). Equations of linear WHP/SSP graphs Y = A + B·X, where X and Y are quantities shown in horizontal and vertical axes, respectively, are shown. Other designations are given in the text of the paper and the Supplementary Materials Section S2..

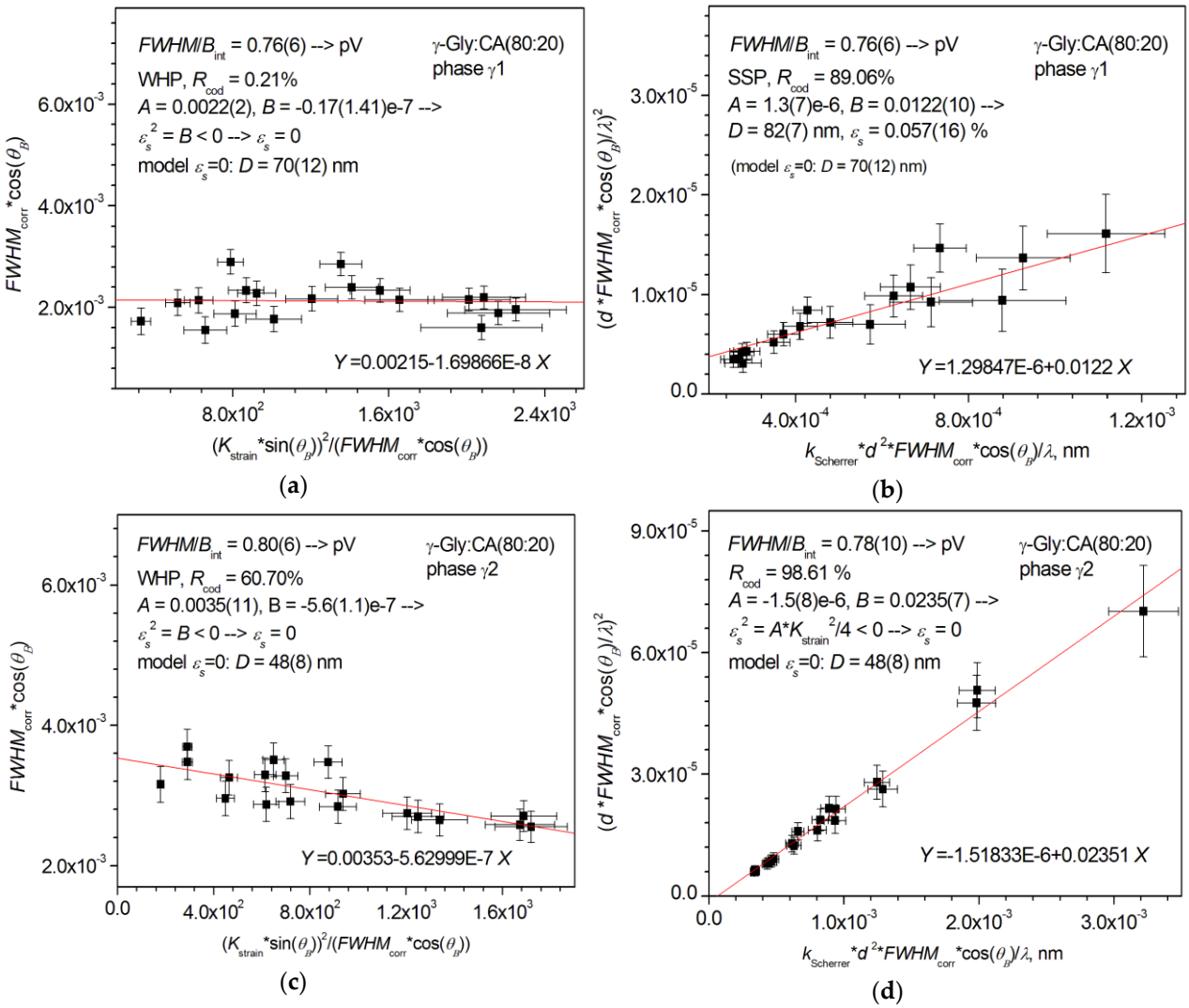

Figure S3. (**a**), (**c**) WHP and (**b**), (**d**), (**f**) SSP of γ1 and γ2 modifications of γ-Gly. For other information see caption to Figure S2.

The LB and Rietveld fittings and refinement were carried out using Rietveld program TOPAS, version 5 (Bruker AXS, Karlsruhe, Germany).

To confirm the LPA results and to obtain more precise parameter values, the XRD patterns were fitted using LB method with refinement of the parameters of the unit cells of the phases and their microstructural parameters. The space groups established in the single-crystal study were used. The parameters of the unit cells of the phases and their microstructural parameters obtained in LPA were taken as initial data.

In turn, in order to check how well the structural models obtained in the single-crystal study (Table 1 of the paper main text) describe the measured XRD powder patterns α-Gly:CA(90:10) and γ-Gly:CA(80:20), the next step was the fitting of XRD patterns by the Rietveld method. In the Rietveld method, the reflection intensities of both phases in each of the studied samples were calculated by the Rietveld program TOPAS, based on the structural model determined in the single-crystal study in this paper. The coordinates of the atoms obtained in the single-crystal study were not refined in the Rietveld fitting at first stage. The parameters of the unit cells of the phases and their microstructural parameters obtained in LB fitting were taken as starting points for refinement.

The background in LeBail (LB) and Rietveld fittings was described by the Chebyshev polinom of 6th order with additional contribution of hyperbolic component to describe better the small-angle (2θ < ~10^{o}) region. The FP (first principles, fundamental parameters) type of XRD reflection profiles was used for LB and Rietveld fittings. The description of the reflection profiles as FP-type profiles makes it possible to calculate the instrumental broadening of reflections based on the fundamental parameters of the diffractometer (geometry, slit sizes, *etc.*) and to refine the microstructure parameters (the average size of crystallites and the absolute value of the average micro-strain) to account for the remaining broadening of reflections.

During the Rietveld structure refinement, the atomic overall temperature factors $U_{iso}^{overall}$ for every sort of atoms were refined but not together with parameters of the preffered orientation in order to prevent the correlation between the parameters being refined.

The final agreement factors characterizing the quality of LB and Rietveld fittings are summarized in Table 7 of the main text of the paper. It should be noted that the agreement factors cR_{wp} and cR_p after subtracting the background contribution were not taken from the output of the TOPAS program (R_{wp}' and R_p' factors in the TOPAS output), but were calculated by the RietESD program. As shown in the examples in [5], in the case of using a hyperbolic background component in a small-angle 2θ region (Figure 2 and Supplementary Materials Figures S4 and S5), as for XRD patterns of the studied samples, TOPAS gives underestimated values of these factors.

The graphical results of LB fitting are presented in Figure S4. The graphical results of Rietveld fitting performed with refinement of atomic coordinates of phases are presented in Figure S5.

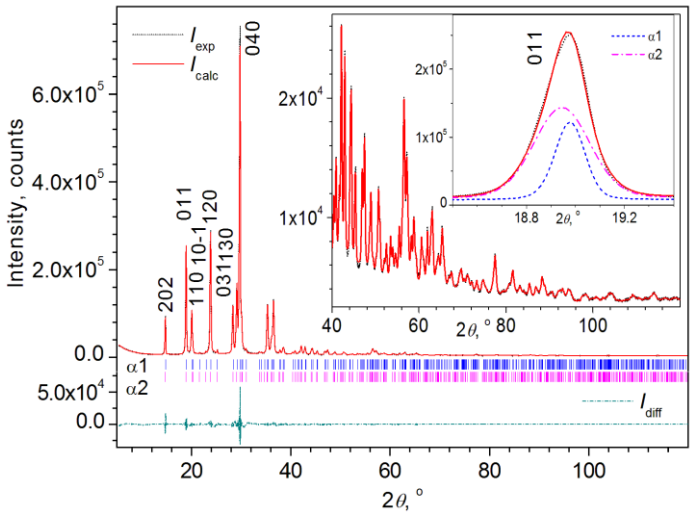

(**a**)

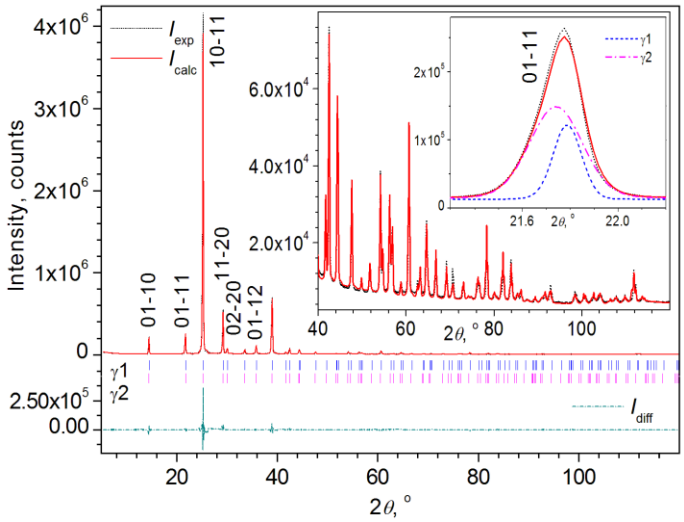

(**b**)

Figure S4. LB fit results for (**a**) α-Gly:CA(90:10 and (**b**) γ-Gly:CA(80:20). The Miller indices *hkl* and Miller-Bravais indices *hkil* of some selected reflections are indicated in (**a**) and (**b**), respectively. Large insets in (**a**, **b**) show the quality of fitting the high 2θ angle regions of the XRD patterns in a larger scale. Examples of LB fitting the asymmetric non-overlapping reflections are shown.

A comparison of the results given in Tables 2, 3 and 6 of the paper main text shows that the parameters and volume of the unit cell of the phase designated as α1 in the powder α-Gly:CA(90:10) (measurements at 313 K) are close to the values found in studies of α-Gly:CA(90:10) single crystals and to the literature data for pure α-Gly at room temperature (*cf.* V_{cell} = 309.85(9) Å^3 in α1 (LB fit) and 309.43(5) Å^3 in α-Gly:CA(90:10) single crystal, and 310.10(4) Å^3 and 309.00(3) for pure α-Gly). In the case of γ-Gly:CA(80:20), the difference in the values of the parameters and V_{cell} of unit cells in powder and single-crystal samples is obviously related to the significantly different temperatures of single-crystal (100 K) and powder (313 K) XRD experiments. However, there is a similarity of their values with the literature data for pure γ-Gly at room temperature, (*cf.* V_{cell} = 231.30(2) Å^3 in γ-Gly:CA(90:10) single crystal, 235.40(12) Å^3 in γ1 (LB fit), and 235.15(3) Å^3 and 235.280(6) for pure γ-Gly at RT [1, 6]).

The values of the agreement coefficients obtained with the LB fit are only ~1.5% less than with the Rietveld fit (Table 7 of the paper main text). Since the quality achieved in LB fitting is close to the maximum possible with Rietveld fitting, it is unlikely that the refinement of atomic coordinates in the Rietveld method will lead to a significant decrease in the values of agreement factors. Indeed, in the case of α-Gly:CA(90:10), the refinement of the coordinates of the atoms allowed to reduce the R_{wp} by only less than 1% (when refining the atomic coordinates, the restrictions on the values of the interatomic distances were applied that they do not deviate from the values obtained from single crystal structure model by more than ~0.1 Å for distances smaller than ~2 Å (~0.2 Å for distances > ~2 Å). The graphical results (Figure S5) at the same time are practically indistinguishable from the results obtained without refinement of the atomic coordinates (Figure 2 of the main text of the paper).

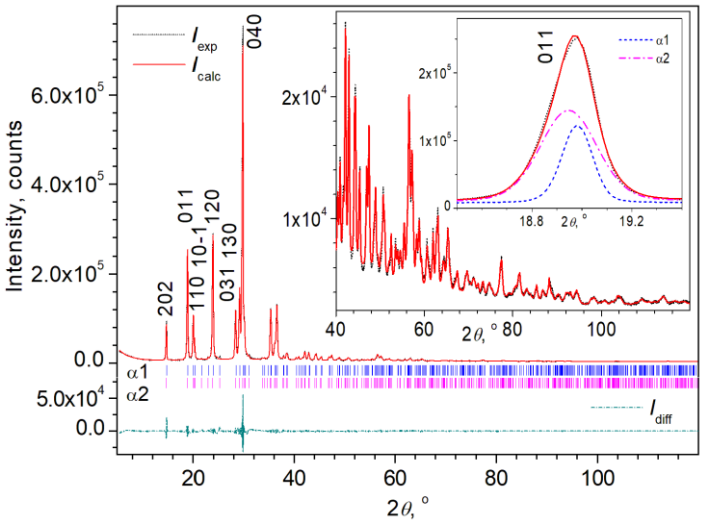

Figure S5. Rietveld fit results for α-Gly:CA(90:10). During the fit the atomic coordinates of the phases were refined. The Miller indices *hkl* of some selected reflections are indicated. Large inset shows the quality of fitting the high 2θ angle region of the XRD pattern in a larger scale. Example of Rietveld fitting the asymmetric non-overlapping reflection is shown.

S3. Raman spectroscopy

Comparison of frequencies of Raman lines observed CA doped α- and γ-Gly crystals [7] and in pure glycine crystals [8,9].

Table S5. Low frequency intermolecular modes and symmetry modes in Gly:CA plate in different experimental geometries, and in nominally pure α-Gly [7].

N	X(ZZ)X	X(YY)X	X(YZ)X	α-Gly [7]	Symmetry
1	50 s	51 s	53 w	52	Ag
2	–	–	71 s	73	Bg
3	99 s	100 s	–	110	Ag
4	154s	–	–	155	Ag
5	–	–	178 m	178	Bg
6	196 m	197m	–	–	Ag

Table S6. High frequency intramolecular modes in Gly:CA plate in different experimental geometries, and in nominally pure α-Gly [8].

N	X(ZZ)X	X(YY)X	X(YZ)X	α-Gly [8]	assignment
1	2971 s	2973 s	2973 s	2973	$\nu_s CH_2$
2	3008 s	3007 s	3009 s	3008	$\nu_a CH_2$

Table S7. Low frequency intermolecular modes in Gly:CA pyramid in different experimental geometries, and in nominally pure γ-Gly [9].

N	Z(YY)Z	Z(*XX*)Z	Z(XY)Z	γ-Gly [9]	assignment
1	85 vs	86 vs	85 vs	89	LM
2	102s	103s	102s	105	LM
3	149.5 s	149.5 s	149.5s	141	LM
4	216m	216m	215m	217	LM

Table S8. High frequency intramolecular modes in Gly:CA pyramid, and in nominally pure γ-Gly [8].

.

N	X(ZZ)X	*X(YY)X*	X(YZ)X	γ-Gly [8]	assignment
1	2963.7s	2963.7 s	2963.7 m	2964	$\nu_s CH_2$
2	2999 s	3000 s	3000 s	3000	$\nu_a CH_2$
3	3100m	3099m	3107m	3098	νNH(3)…O(1)

References

1. Boldyreva, E. V.; Drebushchak, T. N.; Shutova, E. S. Structural distortion of the a, b, and g polymorph of glycine on cooling. *Z. Kristallogr.* **2003**, *218*, 366–376. https://doi.org/10.1524/zkri.218.5.366.20729
2. Farrugia, L. J. ORTEP-3 for Windows - a version of ORTEP-III with a Graphical User Interface (GUI). *J. Appl. Crystallogr.* **1997**, *30*, 565–565. https://doi.org/10.1107/s0021889897003117
3. Levin, A.A. Program *SizeCr* for calculation of the microstructure parameters from X-ray diffraction data. Preprint, **2022**, https://www.researchgate.net/profile/Alexander-Levin-6/research. https://doi.org/10.13140/RG.2.2.15922.89280
4. Balashova, E.; Levin, A. A.; Fokin, A.; Redkov, A.; Krichevtsov, B. Structural Properties and Dielectric Hysteresis of Molecular Organic Ferroelectric Grown from Different Solvents. *Crystals*, **2021**, *11*, 1278. https://doi.org/10.3390/cryst11111278
5. Levin, A.A. Program *RietESD* for correction of estimated standard deviations obtained in Rietveld-refinement program. Preprint, 2022, https://www.researchgate.net/profile/Alexander-Levin-6/research, **2022**, https://doi.org/10.13140/RG.2.2.10562.04800
6. Aree, T.; Bürgi, H.-B.; Chernyshov, D.; Törnroos.K. W. Dynamics and Thermodynamics of Crystalline Polymorphs. 3. γ-Glycine, Analysis of Variable Temperature Atomic Displacement Parameters, and Comparison of Polymorph Stabilities. *J. Phys. Chem. A*, **2014**, *118*, 9951 – 9959. https://doi.org/10.1021/jp506659c
7. Balashova, E. V.; Smirnov, A. N.; Davydov, V.Yu.; Krichevtsov, B. B.; Starukhin, A. N. Raman scattering and luminescence in single crystals of the amino acid glycine $C_2H_5NO_2$ with an admixture of croconic acid $C_5H_2O_5$. *J. Phys. Conf. Ser.* **2021**, *2103*, 012070. https://doi.org/10.1088/1742-6596/2103/1/012070
8. Andrews, B.; Torrie, B. H.; Powell, B. M. Intermolecular potentials for alpha-glycine from Raman and infrared scattering measurements. *Biophys. J.* **1983**, *41*. 293-8. https://doi.org/10.1016/S0006-3495(83)84441-5
9. Baran, J.; Ratajczak, H. Polarised IR and Raman spectra of the γ-glycine single crystal. *Spectrochim. Acta A*, **2005**, *61*, 1611-26. https://doi.org/10.13140/10.1016/j.saa.2004.11.064

.